Talanta 128 (2014) 408–413

Contents lists available at ScienceDirect

Talanta

journal homepage: www.elsevier.com/locate/talanta

Selective and eco-friendly method for determination of mercury(II) ions in aqueous samples using an on-line AuNPs–PDMS composite microfluidic device/ICP-MS system

Keng-Chang Hsu [a], Cheng-Fa Lee [b], Wei-Chang Tseng [c], Yu-Ying Chao [d], Yeou-Lih Huang [a,b,e,*]

[a] Graduate Institute of Medicine, Kaohsiung Medical University, Kaohsiung 80708, Taiwan
[b] Department of Medical Laboratory Science and Biotechnology, Kaohsiung Medical University, Kaohsiung 80708, Taiwan
[c] Department of Medical Laboratory Science and Biotechnology, Fooyin University, Kaohsiung 80708, Taiwan
[d] Department of Public Health, College of Health Science, Kaohsiung Medical University, Kaohsiung 80708, Taiwan
[e] Center of Excellence for Environmental Medicine, Kaohsiung Medical University, Kaohsiung 80708, Taiwan

ARTICLE INFO

Article history:
Received 14 February 2014
Received in revised form
2 May 2014
Accepted 5 May 2014
Available online 14 May 2014

Keywords:
Polydimethylsiloxane
Gold nanoparticle
Mercury
Microfluidics
Inductively coupled plasma mass spectrometry

ABSTRACT

In this study we developed an on-line, eco-friendly, and highly selective method using a gold nanoparticle (AuNP)-coated polydimethylsiloxane (PDMS) composite microfluidic (MF) chip coupled to inductively coupled plasma mass spectrometry (ICP-MS) to separate trace Hg^{2+} ions from aqueous samples. Because Hg^{2+} ions interact with AuNPs to form Hg–Au complexes, we were able to separate Hg^{2+} ions from aqueous samples. We prepared the AuNPs–PDMS composite through *in situ* synthesis using a PDMS cross-linking agent to both reduce and embed AuNPs onto PDMS microchannels so that no additional reductants were required for either AuNP synthesis or the PDMS surface modification (2% $HAuCl_4$, room temperature, 48 h). To optimize the proposed on-line system, we investigated several factors that influenced the separation of Hg^{2+} ions in the AuNPs–PDMS/MF, including adsorption pH, adsorption and elution flow rates, microchannel length, and interferences from coexisting ions. Under optimized conditions (pH 6.0; adsorption/elution flow rates: 0.05/0.5 mL min^{-1}; channel length: 840 mm), we evaluated the accuracy of the system using a standard addition method; the measured values had agreements of $\geq$93.0% with certified values obtained for Hg^{2+} ions. The relative standard deviations of the proposed method ranged from 2.24% to 6.21%. The limit of detection for Hg^{2+} for the proposed on-line AuNPs–PDMS/MF/ICP-MS analytical method was as low as 0.07 μg L^{-1}.

1. Introduction

Microfluidic (MF) technology is attracting increasing attention because it is characterized by inexpensive fabrication, low consumption of sample and reagents, short reaction times, and high sample throughput. Several MF platforms have demonstrated great potential as suitable tools for biological and chemical analyses [1–3]. However, the applications of MF techniques for the analyses of trace elements are currently quite nascent. For trace element analysis, some MF-based techniques [4–6] illustrate the potential of using polymer-based MF techniques for the analysis of trace elements. In a previous study, we developed an on-line polymer-based MF device coupled to ICP-MS for chromium speciation [7].

Various polymers have been applied to prepare MF devices including poly(methyl methacrylate) (PMMA), polyvinylchloride (PVC), polycarbonate (PC), and polydimethylsiloxane (PDMS); the latter has been particularly useful because of its biocompatibility, nontoxicity, thermal and oxidative stability, ease of fabrication, and ability to be sealed with various materials [8–11]. However, the $OSi(CH_3)_2$ groups in PDMS create a hydrophobic surface, resulting in poor wettability with aqueous solutions, making it difficult to introduce aqueous solutions [12]. As a result, chemical modification and physical masking have been used to modify PDMS surfaces to increase their hydrophilicity [13–15]. Metal nanoparticles (NPs) have been used to increase the surface polarities of polymeric matrices can effectively tailor the surface energies of PDMS materials. However, the fine sizes of nanomaterials also mean that the NPs used to adsorb analytes in aqueous

* Corresponding author at: Department of Medical Laboratory Science and Biotechnology, Kaohsiung Medical University, No. 100, Shih-Chuan 1st Road, Kaohsiung 807, Taiwan. Tel: +886 7 312 1101x2251; fax: +886 7 311 3449.
E-mail address: yelihu@kmu.edu.tw (Y.-L. Huang).

http://dx.doi.org/10.1016/j.talanta.2014.05.010
0039-9140/

samples are difficult to recover. This problem can be overcome by immobilizing nanomaterials onto various substrates to act as immobilization matrices and separation tools. Different nanoparticles such as gold and titanium nanoparticles have been deposited on PDMS surfaces for the determination of various analytes [16–20]. The coupling of the multifunctional PDMS with different substrates such as nanoparticles diversifies its applicability for biological and chemical analytes.

Mercury (Hg) is a naturally occurring element that plays important roles in many industrial and agricultural applications; unfortunately, it is also one of the most toxic elements affecting human health. Accordingly, the World Health Organization (WHO) has set the guideline value for inorganic Hg in drinking water at 0.006 mg L^{-1} [21]. One of the most sensitive technique for the detection of Hg and its species is inductively coupled plasma mass spectrometry (ICP-MS) is particularly attractive because of its excellent performance and amenability for coupling with various sample preparation methods [22–25]; however, the need for large amounts of samples and harmful reagents is a drawback. Several analytical methods for the detection of Hg have been investigated as simpler and greener alternatives [26–30].

Although many analytical methods for AuNP-based detection of trace elements have been published during the last decade, of AuNP-modified PDMS MF devices used as solid phase adsorbents for both the preconcentration and determination of trace elements. In this study, our aim was to develop an eco-friendly and on-line system using a AuNPs-modified PDMS composite microfluidic device coupled to ICP-MS for the preconcentration and determination of mercury ions in aqueous samples. The *in situ* synthesis of the AuNPs–PDMS composite was simple and green, and did not require additional reagents other than the curing agent. The proposed method was able to minimize contamination, remove unwanted sample matrix, and simplify the analytical procedure. Several parameters that affected the adsorption efficiency of the AuNPs–PDMS composite were optimized and validated.

2. Experimental

2.1. Materials

A Sylgard 184 PDMS elastomer kit (part A: PDMS monomer; part B: curing agent) was purchased from Dow Corning Company (Midland, MI, USA). Tetrachloroauric acid trihydrate ($HAuCl_4 \cdot 3H_2O$), ultra-pure nitric acid (HNO_3), and hydrochloric acid (HCl) were purchased from Sigma-Aldrich (St. Louis, MO, USA). Mercury(II) nitrate and L-cysteine were purchased from Merck (Darmstadt, Germany). Deionized water (18.3 MΩ cm), prepared using a Barnstead nano-pure water system (Dubuque, IA, USA), was employed throughout this study. All trace element standards and chemicals were of analytical grade and used without further purification. To avoid contamination, all connection tubing was made of polytetrafluoroethylene (PTFE) and flushed with HCl and deionized water prior to use. The chip outlet was connected to the nebulizer of the ICP-MS instrument at a desired flow rate.

2.2. Fabrication and modification of PDMS–AuNPs composite MF device

To synthesize the PDMS plate, the PDMS monomer (part A) and the curing agent (part B) were mixed in a 10:1 ratio (*m*/*m*) and then cured at 60 °C for 120 min. The microchannels of the resulting PDMS plate were designed using CorelDraw9 software and fabricated through etching with a CO_2 laser (Venus, GCC, Taipei, Taiwan). Fig. 1 provides a schematic representation of the layout of the proposed PDMS device. The MF device was comprised of two PDMS layers (15 mm × 60 mm) – one with a microchannel, and the other with two access holes (diameter: 0.2 mm) acting as the sample inlet and outlet. Both layers were cleaned with water, dried in an incubator, and then sealed together to form the reversible PDMS MF device.

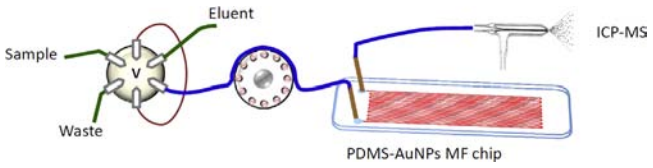

Fig. 1. Schematic representation of the on-line AuNPs–PDMS/ICP-MS system.

The channel interior of the PDMS-based MF device was modified with AuNPs through *in situ* synthesis, exploiting the reductive properties of the residual Si–H groups in the PDMS matrix [18,33]. The MF device was first flushed with deionized water, after which a peristaltic pump was used to introduce 2% (*m*/*v*) $HAuCl_4$ solution into the microchannels. To avoid evaporation of the $HAuCl_4$ solution, the inlet and outlet were sealed. After the microchannels were coated with AuNPs, they were flushed with deionized water to remove residual $HAuCl_4$ solution. Prior to use, the modified PDMS MF device was filled with deionized water and stored at room temperature. This AuNPs–PDMS composite MF device has a long shelf-life of several months if stored at 4 °C [19]. The AuNPs–PDMS MF device was connected to the ICP-MS apparatus through an FI system. PTFE tubing was used to connect the six-port valve to the inlet of the MF device, and the outlet of the MF device to the ICP-MS sampling tube. To avoid contamination, the on-line MF/ICP-MS system was pre-cleaned with deionized water and L-cysteine prior to detection of Hg.

2.3. AuNPs–PDMS/MF/ICP-MS procedures

The AuNPs–PDMS/MF device was connected directly to the ICP-MS system through a six-port valve (Fig. 1). For experiments with on-line determination, a time-resolved mode of data acquisition (TRA) was used to obtain a chromatogram. The use of the on-line AuNPs–PDMS/MF/ICP-MS system for the determination of Hg^{2+} ions involved three steps. First, for sample loading, an aliquot (20 μL) of the sample solution was introduced into the sample inlet reservoir through a six-port injector equipped with a polyether ether ketone (PEEK) sample loop (20 μL). Second, for sample injection, the sample solution was passed through the AuNPs–PDMS MF device such that the Hg^{2+} ions adsorbed onto the AuNPs–PDMS composite. Third, for sample elution, the adsorbed Hg^{2+} ions were eluted using a solution of L-cysteine; the effluent was introduced directly into the ICP-MS instrument for the detection of Hg. The operating conditions of the ICP-MS in the on-line procedure are summarized in Table 1.

2.4. Validation and applications

Environmental water samples were tested to verify the practicality of the AuNPs–PDMS/MF device. Tap water samples were collected from Kaohsiung Medical University. Aliquots were placed into pre-cleaned perfluoroalkoxy (PFA) screw-cap bottles, passed through a 0.45-μm membrane filter, and then analyzed separately using the on-line system. To validate the accuracy of the proposed method, a spike recovery test and the analysis of a certified reference material (NIST 1641d, mercury in water) were performed. All experiments were performed in triplicate to ensure reliability.

Table 1
Operating conditions for the on-line AuNPs–PDMS/MF/ICP-MS system.

ICP-MS parameters	
Instrument	Thermo X Series-II
RF power, W	1280
Auxiliary flow, L min^{-1}	0.88
Nebulizer gas flow, L min^{-1}	0.97
Interface	Ni sample cone (0.75 mm orifice) Ni skimmer cone (0.75 mm orifice)
Measured isotopes	^{200}Hg, ^{202}Hg
Dwell time, ms	500
Duration time, s	360
AuNPs–PDMS composite–MF parameters	
Sample loop, μL	20
Eluent	10 mM L-cysteine
Flow rate, mL min^{-1}	
Adsorption	0.05
Elution	0.5

3. Results and discussion

3.1. Characterization of PDMS–AuNPs composite

Based on a previous study, it was found that no additional reducing agent was required for the reduction of gold ions mediated by the PDMS cross-linking agent [18]. Fig. 2a displays an optical microscopy (ZEISS Primo star, Germany) image of the microchannel cross-section of the AuNP-coated PDMS composite MF device. We also characterized the AuNP-coated PDMS composite through UV–vis spectrophotometry (Jasco V-550, Japan), where we prepared the samples by immersing separate PDMS films in 2% $HAuCl_4$ solution for 24, 48, 72, and 168 h. Fig. 2b displays the UV–vis spectrum of the PDMS film that was incubated in $HAuCl_4$ solution for 48 h. The spectrum of the film features a maximum absorbance wavelength of 556 nm representing the surface plasmon band of the AuNPs. During the preparation of the AuNPs–PDMS composite films, we expected several factors to affect the kinetics of the reaction between $HAuCl_4$ and the PDMS cross-linking agent, including the concentration of $HAuCl_4$ and the incubation time and temperature. As described by SadAbadi et al. [20], a higher concentration of the gold salt led to a higher number of particles formed in a unit area, therefore increasing the absorbance. In this study, we observed the same phenomenon spectrophotometrically, where the absorbance of the PDMS film was higher when the concentration of $HAuCl_4$ was 2% than it was at 1% (data not shown). As a result we employed 2% $HAuCl_4$ throughout the study. The intensity of the absorbance of the AuNPs–PDMS film also increased with the incubation time, indicating an increase of the number of AuNPs on the PDMS film [29,31]. Fig. 2c displays the photographs of a microchannel PDMS MF device before and after incubation with 2% aqueous $HAuCl_4$ for 48 h. The color of the PDMS microchannel treated $HAuCl_4$ for 48 h at room temperature was pale red, but became violet red when the reaction time was extended to 168 h. Such a prolonged reaction time would however lead to aggregation of AuNPs and therefore negatively affect their adsorption efficiency. Thus, we selected an incubation time of 48 h for our following experiments. We also examined the effect of the incubation temperature on the coating efficiency of the AuNPs. Although an increase in the incubation temperature significantly decreased the time required to form the AuNPs, preparation of the AuNPs–PDMS composite in the microchannel at an elevated temperature (60 °C) resulted in the evaporation of the $HAuCl_4$ solution; therefore, we prepared this composite at room temperature for our following experiments. After *in situ* synthesis, UV spectrophotometry was used to evaluate the stability of AuNPs onto the PDMS substrate. AuNPs–PDMS films were immersed into 5% HNO_3 for 24, 48, and 72 h. After a certain time, the AuNPs–PDMS films were washed with deionized water and then analyzed by a UV spectrophotometer. Based on our results, there were no significant differences on the absorbance between treated times.

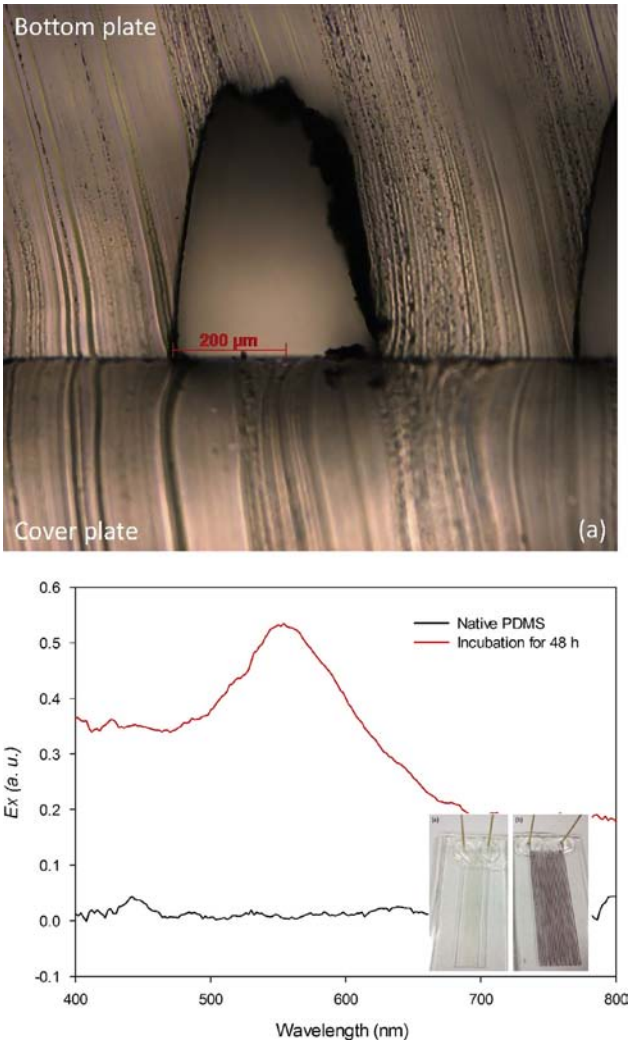

Fig. 2. (a) Photograph of the cross-section of a microchannel in a AuNP-coated PDMS composite MF device. (b) UV–vis spectra of a PDMS film incubated in 2% $HAuCl_4$ solution for various incubation times. (c) Photographs of a PDMS-based MF device before and after incubation with $HAuCl_4$.

3.2. Effect of the adsorption and elution pH

Since pH is one of the most important factors affecting adsorption efficiency, we examined the influence of the pH of the sample solution on the sorption of Hg^{2+} ions in our device by adjusting the pH of the solutions from 3.0 to 11.0. Fig. 3a reveals that increasing the pH from 3.0 to 6.0 increased the adsorption efficiency, but further increase from pH 6.0 to 8.0 resulted in a gradual decrease in adsorption efficiency. Furthermore, we observed no obvious adsorption of Hg^{2+} ions when we increased the pH from 8.0 to 11.0. As described by Wang et al. [30], Hg^{2+} ions form various species (*e.g.*, HgO) at pH values greater than 7.0 that inhibit the formation of Hg–Au complexes. Accordingly, we selected a pH of 6.0 as the optimal value for our subsequent experiments.

In Hg separation methods based on solid phase preconcentration, various strategies can be adopted to elute the Hg species from

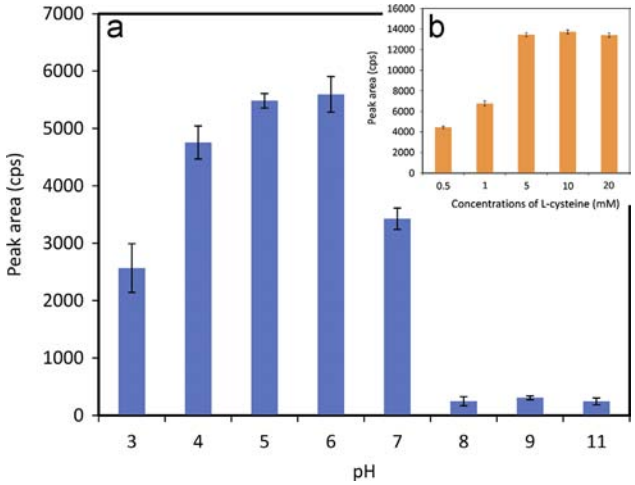

Fig. 3. (a) Effect of pH on the rate of adsorption (%) of Hg^{2+} ions by a AuNPs–PDMS composite MF device. Sample volume: 20 μL; concentration: 1.0 μg L^{-1}. (b) The effect of L-cysteine concentration on the elution of Hg^{2+}.

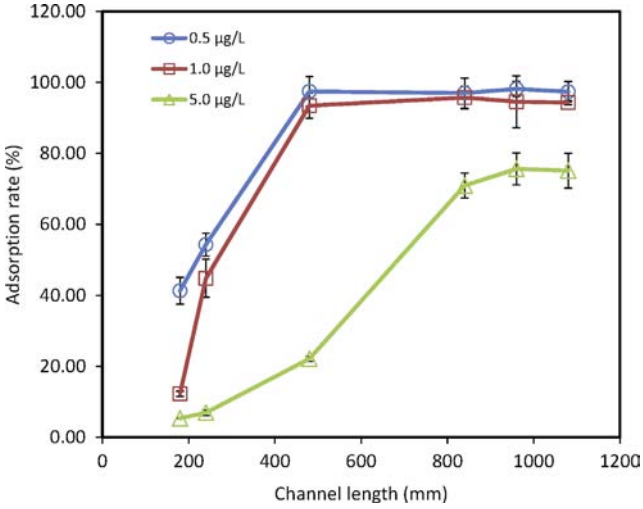

Fig. 4. Effect of microchannel length (180, 240, 480, 840, 960, or 1080 mm) on the adsorption of Hg^{2+} ions. Sample volume: 20 μL; concentration: 0.5, 1.0, or 5.0 μg L^{-1}. The adsorption rates were calculated as follows: Adsorption rate (%)= $[(Conc._{initial} - Conc._{residual})/Conc._{initial}] \times 100\%$.

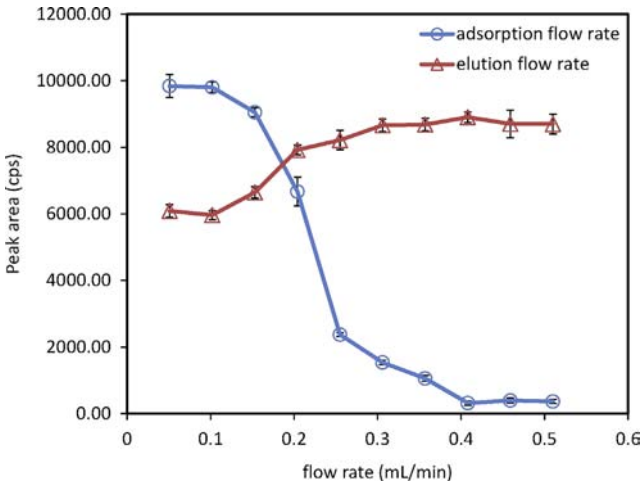

Fig. 5. Effects of flow rates on the adsorption and elution of Hg^{2+} ions in the AuNPs–PDMS composite MF device. Adsorption and elution flow rates: 0.05, 0.1, 0.15, 0.2, 0.25, 0.3, 0.35, 0.4, 0.45, and 0.5 mL min^{-1}. Sample volume: 20 μL; concentration: 1.0 μg L^{-1}; eluent: 10.0 mM L-cysteine.

their complexes, including changing the pH or adding a sulfur-containing ligand. Hence, we evaluated the elution efficiency in the presence of HCl, HNO_3, and L-cysteine, respectively. Although HCl and HNO_3 exhibited good efficiencies for the elution of Hg^{2+} ions, the use of inorganic acids as washing solution required long analyte washout times, which affected the accuracy and reliability of the analytical procedure. As a result, L-cysteine was found to improve the elution efficiency of Hg^{2+} ions. We suspected that the formation of Hg–S bonds with L-cysteine was responsible for the removal of Hg^{2+} ions from the surface of the AuNPs–PDMS composite. According to Li et al. [32], L-cysteine has a strong affinity toward Hg and can be used to eliminate memory effects of Hg in analytical systems. Subsequently, we examined the effects of various concentrations of L-cysteine (0.5, 1.0, 5.0, 10.0, 20.0 mM) on the complete desorption of Hg^{2+} ions. Fig. 3b reveals that L-cysteine concentrations lower than 10.0 mM led to a decrease in the peak area of Hg^{2+}, indicating poorer elution efficiency. Hence, we selected 10.0 M L-cysteine as our eluent for subsequent experiments.

3.3. Effect of microchannel length and adsorption and elution flow rates

Fig. 4 displays the effect of the microchannel length of the MF device on the adsorption rate of Hg^{2+}. We evaluated the effects of different microchannel lengths ranging from 180 to 1080 mm on the adsorption of Hg^{2+} ions from standard solutions (at concentrations of 0.5, 1.0, and 5.0 μg L^{-1}). The adsorption efficiency of the Hg^{2+} ions was found to increase with the microchannel length. However, when we used a microchannel length of 1080 mm and a test solution containing 5.0 μg L^{-1} of Hg^{2+}, we obtained an adsorption of only 75.14%, where the concentration of Hg^{2+} ions may have exceeded the adsorption capacity of the AuNPs–PDMS composite microchannel. Although increasing the channel length did increase the adsorption capacity, it also increased the analysis time. As a result, we selected a microchannel length of 840 mm for our subsequent experiments.

The influence of both adsorption and elution flow rates from 0.05 to 0.5 and 0.05 to 0.6 mL min^{-1}, respectively, on the adsorption efficiency of the AuNPs–PDMS chip was also investigated. Fig. 5 indicates that an adsorption flow rate of 0.05 mL min^{-1} yielded the highest adsorption efficiency of Hg^{2+}, where further increases in the flow rate yielded lower adsorption efficiencies. On the other hand, elution flow rates ranging from 0.3 to 0.5 mL min^{-1} had no obvious influence on the desorption efficiencies of Hg^{2+}. In conclusion, the adsorption and elution flow rates chosen for subsequent experiments were 0.05 and 0.5 mL min^{-1}, respectively.

3.4. Performance of the on-line AuNPs–PDMS/MF/ICP-MS system

We investigated the analytical performance of our on-line AuNPs–PDMS/MF/ICP-MS system under the optimized conditions. To verify the selectivity of the developed method for the determination of Hg^{2+} ions in aqueous samples, we also tested the effects of coexisting ions on the recovery of Hg^{2+} ions, where we mixed 1.0 μg L^{-1} Hg^{2+} with 100 μg L^{-1} of Ca^{2+}, Cd^{2+}, Co^{2+}, Cr^{3+}, Cu^{2+}, K^{+}, Mg^{2+}, Na^{2+}, Ni^{2+}, Pb^{2+}, and Zn^{2+}. The results showed that the recoveries were in the range of 97.5–101.7%, which mean that interferences from coexisting ions can be ignored under the optimal conditions. The concentration–response relationship of the present analytical method indicated linearity over the concentration range 0.2–4.0 μg L^{-1} with a correlation coefficient of 0.9992. The limit of detection (0.07 μg L^{-1}) was estimated from seven replicate measurements as equivalent to three times the

standard deviation of the background signal. On the other hand, the determination of Hg by ICP-MS is typically hindered by severe memory effects. The residual analytes inside the system, which not only affects the subsequent measurement but also the accuracy and reliability of the analytical procedure and the reusability of the AuNPs–PDMS device. Therefore, an additional cleaning step (5% HNO_3 for 1 min) was used to elute residual analytes between each analytical run, where a flow rate of 1.0 mL min^{-1} for 1 min was able to reduce the memory effects. Furthermore, the reusability of AuNPs–PDMS chip was checked using the same procedure for sorption–desorption of Hg^{2+} ions. Based on our results, the AuNPs–PDMS chip could be reused up to 30 adsorption/elution cycles without any changes in performance.

The applicability of this developed system for the analysis of nature water samples was also investigated. Aliquots of tap water and environmental water samples were collected from Kaohsiung city and stored in pre-cleaned PFA screw-cap bottles, passed through a 0.45-μm membrane filter, and analyzed using our on-line AuNPs–PDMS/MF/ICP-MS system. Table 2 reveals that the recoveries for Hg^{2+} spikes from 0.2 to 1.0 μg L^{-1} in tap water and environmental water samples ranged from 88.2% to 103.5%. Due to the extremely low concentrations of mercury in natural waters [26] (usually in pg L^{-1} to ng L^{-1} levels), the standard addition method was used to assess the accuracy and precision of the developed method. A diluted certified reference material (NIST SRM1641d, mercury in water) was also used to validate the proposed method. The results were in reasonable agreement with the measured and spiked values of the water samples. Table 3 compares the figures of merit of the proposed method with those of other methods for the determination of Hg^{2+} ions [33–39]. Relative to typical analytical systems, MF chip-based techniques for trace element analysis are simpler and decrease reagent consumption, waste production, and reaction times.

Table 2
Assay results for environmental aqueous samples and certified reference materials analyzed using the proposed AuNPs–PDMS/MF/ICP-MS system.

Sample	Certified value (μg L^{-1})	Observed value (μg L^{-1})	Spike recovery (%)
NIST 1641d	1.557[a]	1.51 ± 0.05[a]	–
Tap water	ND[b]	ND	–
	0.5	0.52 ± 0.02	103.5
	1.0	1.01 ± 0.06	101.4
Location 1	ND	ND	–
	0.5	0.45 ± 0.04	90.5
	1.0	1.00 ± 0.03	100.2
Location 2	ND	ND	–
	0.5	0.44 ± 0.03	88.2
	1.0	0.93 ± 0.01	92.8
Location 3	ND	ND	–
	0.5	0.47 ± 0.01	93.1
	1.0	1.01 ± 0.03	101.0
Location 4	ND	ND	–
	0.5	0.50 ± 0.03	100.9
	1.0	0.97 ± 0.01	96.9

[a] Concentration in mg L^{-1}.
[b] ND: Not detected.

4. Conclusion

In conclusion, we have developed a selective and eco-friendly method for the determination of Hg through the on-line coupling of an MF device with ICP-MS. We coated the microchannels of PDMS-based MF devices with AuNPs through *in situ* synthesis to isolate Hg^{2+} ions from sample solutions *via* formation of Au–Hg complexes. To our knowledge, this is the first paper to report the combination of an AuNP-modified PDMS MF device with ICP-MS for the selective determination of Hg^{2+} ions. The chip was found to be reusable for at least 30 analyses with no significant decrease in adsorption efficiency. However, due to limitations in the adsorption capacity of the home-made AuNPs–PDMS MF devices, further studies in the modification and/or functionalization of the channel surfaces may resolve this problem. Future studies will focus on the use of the proposed method for analysis of different samples. Recent MF chip-based methods for trace element analysis have focused on environmental samples. Applications of MF techniques for trace element analysis in biological samples are quite rare due to the complexity of biological matrices, so that sample pretreatment is often necessary. Another major challenge in the development of MF-based analytical methods for biological samples is the speciation of trace elements without changing their

Table 3
Analytical characteristics of the proposed method compared with those previously published.

Matrix	Instrumental method	Hg species	Sample volume (μL)	Detection limit (ng L^{-1})	References
Environmental water	AuNPs–PDMS/MF/ICP-MS	Hg^{2+}	20	70	Present method
Waste water	microHPLC/ICP-MS	Hg^{2+}	20	11	[33]
Ground water		MeHg		23	
Sea water		EtHg		8	
		Phenylmercury		32	
Environmental water	Gold-coated silica adsorbent packed microcolumn-AFS	Total dissolved Hg	7000	0.18	[34]
Seawater	Short column HPLC/ICP-MS	Hg^{2+}	30,000	0.042	[35]
		MeHg		0.016	
		EtHg		0.008	
Liquid cosmetics sample	DLLME/HPLC/ICP-MS	Hg^{2+}	5000	1.3	[36]
		MeHg		7.2	
Tap water	HF/LPME/HPLC/ICP-MS	Hg^{2+}	10,000	110	[37]
River water		MeHg		230	
Estuarine water					
Serum					
Water samples	SPE/HPLC/ICP-MS	Hg^{2+}	100,000	3	[38]
		MeHg			
River water	HPLC/AFS (on-line digestion)	Hg^{2+}	> 100,000	800	[39]
		MeHg		4300	
		EtHg		1400	
		Phenylmercury		800	

charge states during the various necessary sample pretreatment steps. We are currently undertaking further studies into the applicability of MF-based methods for the speciation and analysis of trace elements in biological samples.

Acknowledgments

This study was supported financially by the National Science Council Taiwan (NSC101-2113-M-037-003-MY3).

References

[1] G.B. Salieb-Beugelaar, G. Simone, A. Arora, A. Philippi, A. Manz, Anal. Chem. 82 (2010) 4848–4864.
[2] D. Mark, S. Haeberle, G. Roth, F. von Stetten, R. Zengerle, Chem. Soc. Rev. 39 (2010) 1153–1182.
[3] X. He, Q. Chen, Y. Zhang, J.M. Lin, TrAC Trends Anal. Chem. 53 (2014) 84–97.
[4] H. Wang, Z.K. Wu, Y. Zhang, B.B. Chen, M. He, B. Hu, J. Anal. At. Spectrom. 28 (2013) 1660–1665.
[5] B.B. Chen, B. Hu, M. He, Q. Huang, Y. Zhang, X. Zhang, J. Anal. At. Spectrom. 28 (2013) 334–343.
[6] T.T. Shih, C.H. Lin, I.H. Hsu, J.Y. Chen, Y.C. Sun, Anal. Chem. 85 (2013) 10091–10098.
[7] K.C. Hsu, C.C. Sun, Y.C. Ling, S.J. Jiang, Y.L. Huang, J. Anal. At. Spectrom. 28 (2013) 1320–1326.
[8] J.C. McDonald, D.C. Duffy, J.R. Anderson, D.T. Chiu, H.K. Wu, O.J.A. Schueller, G.M. Whitesides, Electrophoresis 21 (2000) 27–40.
[9] E. Boscaini, M.L. Alexander, P. Prazeller, T.D. Mark, Int. J. Mass Spectrom. 239 (2004) 179–186.
[10] N. Bao, Q. Zhang, J.J. Xu, H.Y. Chen, J. Chromatogr. A 1089 (2005) 270–275.
[11] R. Samy, T. Glawdel, C.L. Ren, Anal. Chem. 80 (2008) 369–375.
[12] S.K. Sia, G.M. Whitesides, Electrophoresis 24 (2003) 3563–3576.
[13] I. Wong, C.M. Ho, Microfluid. Nanofluid. 7 (2009) 291–306.
[14] A. Goyal, A. Kumar, P.K. Patra, S. Mahendra, S. Tabatabaei, P.J.J. Alvarez, G. John, P.M. Ajayan, Macromol. Rapid Commun. 30 (2009) 1116–1122.
[15] J. Zhou, A.V. Ellis, N.H. Voelcker, Electrophoresis 31 (2010) 2–16.
[16] B. Wang, K. Chen, S. Jiang, F. Reincke, W.J. Tong, D.Y. Wang, C.Y. Gao, Biomacromolecules 7 (2006) 1203–1209.
[17] Z.Q. Niu, F. Gao, X.Y. Jia, W.P. Zhang, W.Y. Chen, K.Y. Qian, Colloids Surf. A Physicochem. Eng. Asp. 272 (2006) 170–175.
[18] Q. Zhang, J.J. Xu, Y. Liu, H.Y. Chen, Lab Chip 8 (2008) 352–357.
[19] W.Y. Wu, Z.P. Bian, W. Wang, W. Wang, J.J. Zhu, Sens. Actuators B Chem. 147 (2010) 298–303.
[20] H. SadAbadi, S. Badilescu, M. Packirisamy, R. Wuthrich, Biosens. Bioelectron. 44 (2013) 77–84.
[21] W.H.O., Guidelines for Drinking-water Quality, 4th ed., 2011.
[22] Y. Zhao, J. Zheng, L. Fang, Q. Lin, Y. Wu, Z. Xue, F. Fu, Talanta 89 (2012) 280–285.
[23] L. Laffont, L. Maurice, D. Amouroux, P. Navarro, M. Monperrus, J.E. Sonke, P. Behra, Anal. Bioanal. Chem. 405 (2013) 3001–3010.
[24] K. Leopold, M. Foulkes, P. Worsfold, Anal. Chim. Acta 663 (2010) 127–138.
[25] R.B. Voegborlo, A.A. Adimado, Food Chem. 123 (2010) 936–940.
[26] W.B. Lu, X.Y. Qin, S. Liu, G.H. Chang, Y.W. Zhang, Y.L. Luo, A.M. Asiri, A.O. Al-Youbi, X.P. Sun, Anal. Chem. 84 (2012) 5351–5357.
[27] Y. Date, A. Aota, S. Terakado, K. Sasaki, N. Matsumoto, Y. Watanabe, T. Matsue, N. Ohmura, Anal. Chem. 85 (2013) 434–440.
[28] C.I. Wang, C.C. Huang, Y.W. Lin, W.T. Chen, H.T. Chang, Anal. Chim. Acta 745 (2012) 124–130.
[29] D.D. Tan, Y. He, X.J. Xing, Y. Zhao, H.W. Tang, D.W. Pang, Talanta 113 (2013) 26–30.
[30] A. Zierhut, K. Leopold, L. Harwardt, M. Schuster, Talanta 81 (2010) 1529–1535.
[31] Y. Li, T. Verbiest, I. Vankelecom, J. Membr. Sci. 428 (2013) 63–69.
[32] Y.F. Li, C.Y. Chen, B. Li, J. Sun, J.X. Wang, Y.X. Gao, Y.L. Zhao, Z.F. Chai, J. Anal. At. Spectrom. 21 (2006) 94–96.
[33] A. Castillo, A.F. Roig-Navarro, O.J. Pozo, Anal. Chim. Acta 577 (2006) 18–25.
[34] K. Leopold, M. Foulkes, P.J. Worsfold, Anal. Chem. 81 (2009) 3421–3428.
[35] X.Y. Jia, D.R. Gong, Y. Han, C. Wei, T.C. Duan, H.T. Chen, Talanta 88 (2012) 724–729.
[36] X.Y. Jia, Y. Han, C. Wei, T.C. Duan, H.T. Chen, J. Anal. At. Spectrom. 26 (2011) 1380–1386.
[37] F. Moreno, T. Garcia-Barrera, J.L. Gomez-Ariza, J. Chromatogr. A 1300 (2013) 43–50.
[38] Y.G. Yin, M. Chen, J.F. Peng, J.F. Liu, G.B. Jiang, Talanta 81 (2010) 1788–1792.
[39] J. Margetinova, P. Houserova-Pelcova, V. Kuban, Anal. Chim. Acta 615 (2008) 115–123.